⌘ *Author's Choice*

THE JOURNAL OF BIOLOGICAL CHEMISTRY VOL. 286, NO. 22, pp. 19641–19651, June 3, 2011
© 2011 by The American Society for Biochemistry and Molecular Biology, Inc. Printed in the U.S.A.

The Biflavonoid Amentoflavone Inhibits Neovascularization Preventing the Activity of Proangiogenic Vascular Endothelial Growth Factors*[S]

Received for publication, September 17, 2010, and in revised form, April 4, 2011 Published, JBC Papers in Press, April 6, 2011, DOI 10.1074/jbc.M110.186239

Valeria Tarallo[‡1], Laura Lepore[§1], Marcella Marcellini[¶], Fabrizio Dal Piaz[§2], Laura Tudisco[‡], Salvatore Ponticelli[‡], Frederik Wendelboe Lund[‖], Peter Roepstorff[‖], Augusto Orlandi[**], Claudio Pisano[¶], Nunziatina De Tommasi[§], and Sandro De Falco[‡3]

From the [‡]Angiogenesis Lab and Stem Cell Fate Lab, Institute of Genetics and Biophysics, "Adriano Buzzati-Traverso," 80131 Napoli, Italy, the [§]Department of Pharmaceutical Sciences, University of Salerno, 84084 Fisciano (Salerno), Italy, the [¶]Research and Development Oncology Area, Sigma-Tau s.p.a., Industrie Farmaceutiche Riunite, 00040 Pomezia (Roma), Italy, the [‖]Department of Biochemistry and Molecular Biology, University of Southern Denmark, Campusvej 55, DK-5230 Odense, Denmark, and the [**]Department of Biopathology and Image Diagnostics, Anatomic Pathology Institute, Tor Vergata University, 00133 Roma, Italy

The proangiogenic members of VEGF family and related receptors play a central role in the modulation of pathological angiogenesis. Recent insights indicate that, due to the strict biochemical and functional relationship between VEGFs and related receptors, the development of a new generation of agents able to target contemporarily more than one member of VEGFs might amplify the antiangiogenic response representing an advantage in term of therapeutic outcome. To identify molecules that are able to prevent the interaction of VEGFs with related receptors, we have screened small molecule collections consisting of >100 plant extracts. Here, we report the isolation and identification from an extract of the Malian plant *Chrozophora senegalensis* of the biflavonoid amentoflavone as an antiangiogenic bioactive molecule. Amentoflavone can to bind VEGFs preventing the interaction and phosphorylation of VEGF receptor 1 and 2 (VEGFR-1,VEGFR-2) and to inhibit endothelial cell migration and capillary-like tube formation induced by VEGF-A or placental growth factor 1 (PlGF-1) at low μM concentration. *In vivo*, amentoflavone is able to inhibit VEGF-A-induced chorioallantoic membrane neovascularization as well as tumor growth and associated neovascularization, as assessed in orthotropic melanoma and xenograft colon carcinoma models. In addition structural studies performed on the amentoflavone·PlGF-1 complex have provided evidence that this biflavonoid effectively interacts with the growth factor area crucial for VEGFR-1 receptor recognition. In conclusion, our results demonstrate that amentoflavone represents an interesting new antiangiogenic molecule that is able to prevent the activity of proangiogenic VEGF family members and that the biflavonoid structure is a new chemical scaffold to develop powerful new antiangiogenic molecules.

In the past few years, it has been demonstrated that the proangiogenic members of VEGF family, VEGF-A, VEGF-B, and placental growth factor (PlGF),[4] play a central role in the modulation of pathological angiogenesis (1, 2). VEGFs accomplish their action interacting with two tyrosine kinase receptors, VEGFR-1 and VEGFR-2, also known as Flt-1 and KDR. Pathological neovascularization is a condition associated to many complex diseases such as cancer, atherosclerosis, arthritis, diabetic retinopathy, and age-related macular degeneration (2, 3).

VEGF-A is the most potent proangiogenic factor known showing a crucial stimulating activity on endothelial cells. Indeed, it is the target of the first U. S. Food and Drug Administration-approved antiangiogenic drugs for the therapy of cancer and age-related macular degeneration. Bevacizumab (Avastin), a monoclonal antibody anti-VEGF-A, has been approved for the therapy of metastatic colorectal cancer in combination with chemotherapy (4), whereas pegaptanib (Macugen), an anti-VEGF-A PEGylated aptamer (5), and ranibizumab (Lucentis), a Fab fragment of bevacizumab (6), have been approved for treatment of age-related macular degeneration. Although VEGF-A-targeted therapy has improved cancer survival, many patients are refractory to VEGF-A-targeted therapy, and most patients who initially respond develop resistance (7).

More recently, increasing attention has been addressed to other members of VEGF network involved in angiogenesis modulation. Indeed, the block of VEGFR-1 (8), or of its specific ligand PlGF (9, 10), is sufficient to strongly inhibit pathological angiogenesis in experimental models of pathologies such as cancer, atherosclerosis, arthritis, ocular neovascular diseases, and metastasis formation (11–15), indicating how fine-tuning of the availability of VEGFs and related receptors is required for a correct angiogenesis during pathological conditions. This is also confirmed by data indicating that the up-regulation of PlGF expression provides a tumor escape strategy to anti-VEGF-A therapy (10, 16).

* This work was supported by Associazione Italiana Ricerca sul Cancro Grant 4840 and Telethon Italy Grant GGP08062 (to S. D. F).

[S] The on-line version of this article (available at http://www.jbc.org) contains supplemental "Experimental Procedures," "Results," Tables S1–S3, and Figs. S1–S10.

⌘ *Author's Choice*—Final version full access.

[1] Both authors contributed equally to this work.

[2] To whom correspondence may be addressed. E-mail: fdalpiaz@unisa.it.

[3] To whom correspondence may be addressed: Angiogenesis LAB, Institute of Genetics and Biophysics "Adriano Buzzati-Traverso," Consiglio Nazionale delle Ricerche, Via Pietro Castellino 111, 80131 Napoli, Italy. Tel.: 39-081-6132354; Fax: 39-081-6132595; E-mail: defalco@igb.cnr.it.

[4] The abbreviations used are: PlGF-1, placental growth factor 1; VEGFR-1, VEGF receptor 1; CTF, capillary-like tube formation; HUVEC, human umbilical vein endothelial cell; AF, amentoflavone; RP, reverse phase.

It appears evident that due to the strict biochemical and functional relationship between VEGFs and related receptors (17), the development of a new generation of agents able to target contemporarily more than one member of the VEGFs might amplify the antiangiogenic response. This would overcome some of the difficulties associated with current angiogenesis inhibitors, representing an advantage in terms of therapeutic outcome (17, 18).

From this perspective, we have performed a screening plan of small molecule collections consisting of >100 extracts from plants used in the traditional medicine collected in various areas of the world. Medicinal plants have become extremely important in drug discovery for the treatment of human diseases, and their secondary metabolites have proven to be the most reliable source of new and effective anticancer agents (19). Moreover, the management of small molecules still offers numerous advantages over biotherapeutics because they can be more easily and cheaply produced. In addition small molecules are more stable and generally free of contaminants of biological origin and may offer more opportunity for delivery.

The screenings have been performed using competitive dose-dependent ELISA assays for PlGF-1 and VEGF-A interaction with high affinity receptor VEGFR-1 (20, 21). The chloroform/methanol extract from leaves of the Malian plant *C. senegalensis* showed the highest inhibiting activity and its subsequent bioassay-guided fractionation led to the isolation and characterization of amentoflavone (AF) as bioactive constituent able to inhibit the interaction of either PlGF-1 or VEGF-A with VEGFR-1. AF belongs to a unique class of naturally occurring biflavonoids (22).

The binding properties and the antiangiogenic activity of the selected compound have been assessed in *in vitro* and cell-based assays. The data presented here demonstrate that AF specifically binds to VEGFs, preventing the activation of both VEGFR-1 and VEGFR-2. It is able to significantly inhibit growth and neoangiogenesis in two different tumor models, an orthotropic model of melanoma and a xenograft model of colon carcinoma.

EXPERIMENTAL PROCEDURES

Materials—Analytical grade solvents were obtained from Carlo Erba (Milano, Italy). HPLC grade acetonitrile (CH_3N), methanol (MeOH), and formic acid were purchased from J. T. Baker (Baker Mallinckrodt, Phillipsburg, NJ). HPLC grade water (18 mV) was prepared using a Millipore (Bedford, MA) Milli-Q purification system.

Recombinant PlGF-1 protein (amino acids 19–149) (23) produced in *Escherichia coli* in our laboratory was used in all the experiments. The numeration of PlGF-1 residues reported below is related to this sequence with an additional methionine in position 1. This recombinant form of PlGF-1 shows the same activity in terms of receptor binding of that produced by R&D Systems (amino acids 21–149; Minneapolis, MN). All of the other recombinant growth factors, receptors, and antibodies used were from R&D Systems.

Plant Extract Preparation—The air-dried powdered plant material was extracted by exhaustive maceration with solvents at increasing polarity. Source plants and kinds of extracts are reported in supplemental Table S1.

Purification of Amentoflavone—The air-dried powdered leaves of *Chrozophora senegalensis* (1 kg) were defatted with *n*-hexane and extracted successively by exhaustive maceration (3 × 1 liter, for 48 h) with $CHCl_3$, $CHCl_3$-MeOH (9:1) (v/v), and MeOH. The extracts were concentrated under reduced pressure to afford 22.4, 28.4, 23.6, and 104.0 g of dried residues, respectively.

A portion of the $CHCl_3$-MeOH (9:1) (v/v) extract (50.0 g) was partitioned between *n*-BuOH and H_2O to give an *n*-BuOH soluble portion (19.0 g). 5.0 g of this residue were chromatographed over a Sephadex LH-20 column (100 cm × 5 cm) with MeOH as the eluent. A total of 100 fractions were collected (11-ml each). These were combined according to TLC analysis (silica 60 F_{254} gel-coated glass sheets with *n*-BuOH-AcOH-H_2O (60:15:25, v/v/v) and $CHCl_3$-MeOH-H_2O (40:9:1, v/v/v)) to give ten pooled fractions (A–L).

The bioactive fraction E (220 mg), purified by RP-HPLC using CH_3CN-H_2O (55:45, v/v), contained a main component (t_R = 13.0 min) at 90% w/w (200 mg), which was identified successfully as AF by determination of structural properties (supplemental data). It was obtained at a purity of 98.4%, as assessed by RP-HPLC diode array detector on a C_{18}-Luna column (2 × 50 mm, flow rate of 0.2 ml min^{-1}) (Phenomenex). The chromatogram was acquired at 280 nm. The injection volume was 20 μl (0.1 mg/ml). The solvent gradient changed according to the following conditions (solvent A, H_2O + HCOOH 0.1% and solvent B, acetonitrile): 0–1 min, 20% B; 20 min, 70% B; 20–23 min, 70% B, 23–24 min, 9 5% B; 24–30 min 100% B (AF t_R = 14.8 min) (supplemental Fig. S1). Purified AF has been used for all *in vitro* and *in vivo* assays.

Surface Plasmon Resonance Analysis—Surface plasmon resonance analyses were performed on a Biacore 3000 (Uppsala, Sweden) optical biosensor equipped with research-grade CM5 sensor chips, as reported elsewhere (24). Briefly, two separate human PlGF-1, VEGF-A, or Fc-VEGFR-1 chimera surfaces, one human serum albumin or human tubulin surfaces and one unmodified reference surface, were prepared for simultaneous analyses.

Immediately after chip docking, the instrument was primed with water, and the sensor chip surfaces were preconditioned by applying two consecutive 20-μl injections each (at a flow rate of 100 μl/min) of 50 mM NaOH, 10 mM HCl, 0.1% SDS (w/v), and 10 mM H_3PO_4. Data were collected at 2.5 Hz. Proteins (100 μg/ml in 10 mM sodium acetate, pH 5.0) were immobilized on individual sensor chip surfaces at a flow rate of 5 μl/min using standard amine-coupling protocols to obtain densities of 8–12 kilo response units. The AF binding study was performed using a five-point concentration series, typically spanning 0.05–10 μM, and triplicate aliquots of each AF concentration were dispensed into single-use vials. Binding experiments were performed at 25 °C, using a flow rate of 50 μl/min, with a 60 s monitoring of association and a 200 s monitoring of dissociation. Simple interactions were adequately fitted to a single-site bimolecular interaction model ($A + B = AB$), yielding a single K_D. Sensorgram elaborations were performed using the Biaevaluation software provided by Biacore AB.

Competitive ELISA Assays—For competitive ELISA used for the screening of plant extracts and for dose-dependent experiments, see the supplemental data (20, 21, 25). Each point was done in triplicate, and each experiment was repeated twice.

Cell Culture—Human umbilical vein endothelial cells (HUVECs) were grown in standard conditions in endothelial basal medium 2 supplemented with bullet kit (EGM-2) containing hydrocortisone, hFGF-B, VEGF, R3-IGF-1, ascorbic acid, heparin, FBS, hEGF, gentamicin, and amphotericin-B (Cambrex, Charles City, IA).

The cell line overexpressing human VEGFR-1, obtained by stable transfection of human embryonic kidney 293 cells and named 293-hFlt-1, was grown as described elsewhere (25). Human tumor cell lines MeWo (ATCC catalog no. HTB-65, from melanoma) and HCT-116 (ATCC catalog no. CCL-247, from colon carcinoma) were grown in Eagle's minimal essential medium or McCoy's 5a medium, respectively, supplemented with 10% FBS, 2 mM glutamine, and standard concentration of antibiotics.

Cell-based Assays—For receptor phosphorylation assays, HUVECs were starved in absence of growth factors but in the presence of 1% FBS. 293-hFlt-1 cells (25) were starved for 16 h in absence of FBS. To induce VEGFR-1 and VEGFR-2 receptor activation, 20 ng/ml of PlGF-1 or 50 ng/ml of VEGF-A for 10 min were used. AF (2- 25 μM) was added to medium at the same time of inductors. As control, neutralizing anti-PlGF mAb (16D3, Thrombogenics, Leuven, Belgium) or anti-VEGF-A antibody (R&D Systems) were used at ~3 nM.

To detect phosphorylated forms of receptors in Western blot experiments performed following standard procedures, antibodies anti-p-VEGFR-1 (R&D Systems) diluted 1:500 and anti-p-VEGFR-2 (Cell Signaling, Danvers, MA) diluted 1:1000 were used. Normalization was performed using anti-VEGFR-1, 1/500 (Sigma-Aldrich) or anti-VEGFR-2, 1/500 (Santa Cruz Biotechnology, Santa Cruz, CA). The values of densitometry analyses, performed using ImageQuant software (version 5.2, Molecular Dynamics) are shown. Values (%) were calculated as ratio of degree of receptors phosphorylation with respect to the total receptor amounts. The value of 1.0 has been arbitrarily assigned to PlGF-1- or VEGF-A-induced samples. Data are representative of three independent experiments.

For toxicity and proliferation assays, see supplemental data. The chemotaxis assay (26) and capillary-like tube formation assays (21, 25) were performed as described elsewhere (see also supplemental data).

In Vivo Analyses—For chorioallantoic membrane assay, see supplemental data.

For tumor models, MeWo human melanoma cells (5×10^5) were inoculated intradermally in the right flank of 24 8-week-old CD-1 male nude athymic mice (Charles River, Chatillon-sur-Chalaronne, France) by using a 100-μl Hamilton syringe. Then, animals were subdivided into two groups ($n = 9$). Starting 3 days after injection, every group was treated as follows: vehicle, 1% gum acacia in sterile water (i.p.) and AF, 50 mg/10 ml/kg (i.p.) as described previously (27). Mice were sacrificed by CO_2 inhalation 14 days after cell injection and tumor nodules were surgically removed, measured, and weighed.

For xenograft tumor experiments, 5×10^6 HCT-116 colon carcinoma cells were injected subcutaneously in 20 8-week-old CD1 nude athymic mice. After 7 days, when tumors reach a volume between 50 and 100 mm^3, animals were divided into two groups ($n = 8$) and treated with AF or vehicle as described before. Tumor growth was followed by three weekly measurements of tumor diameters with a caliper. Tumor volume (TV) was calculated according to the formula: TV (mm^3) = $d^2 \times D/2$, where d and D are the shortest and the longest diameters, respectively. For ethical reasons, mice were sacrificed when control tumors reached in average a volume of 1500 mm^3, after 14 days of drug treatment.

For animal experiments, the care and husbandry of mice and tumor experimental procedures were in accordance with European Directive 86/609 and with Italian Decreto Legge (D.L.) 116. All experiments were approved by the Institute of Genetics and Biophysics and the sigma-tau veterinarians.

Immunohistochemical analyses were performed on 4-μm-thick deparaffined tumor sections incubated overnight at 4 °C with the following primary antibodies: rat anti-mouse PECAM-1 (anti-CD31; 1:1000; BD Pharmingen, San Jose, CA) and rat anti-mouse F4/80 (1:50; Serotec, Oxford, UK). The staining procedure was continued using specific secondary biotinylated antibody (all from DAKO, Glostrup, Denmark). Slides were counterstained with hematoxylin. Images were recorded with a digital camera Leica DC480 (Milano, Italy). Vessel density was manually measured. Densitometric analysis for F4/80 staining was performed with QwinPro software (Leica). Analyses were performed on five optical fields for each tumor.

Structural Characterization of PlGF-1·AF Complex and Molecular Docking—For UV cross-linking, limited proteolysis, mass spectrometry, and docking analyses (28), see supplemental data.

Statistical Analysis—Data are expressed as mean ± S.E., with $p < 0.05$ considered statistically significant. Differences among groups were tested by one-way analysis of variance; Tukey HD test was used as post hoc test to identify which group differences account for the significant overall analysis of variance. All calculations were carried out using the SPSS statistical package (version 12.1, Chicago, IL). The IC_{50} and LD_{50} have been calculated using linear regression fitted using the least squares method.

RESULTS

Identification of Amentoflavone as Bioactive Compound—Polar and apolar plant extracts (supplemental Table S1) were screened for their ability to inhibit the *in vitro* interaction between PlGF-1 and VEGF-A with VEGFR-1. About 5% of extracts tested by competitive ELISA-based assays met the criteria for activity showing a dose-dependent response on both the ELISAs with an inhibition over 50% at a concentration of 100 μg/ml.

The deconvolution of active extracts was thus performed by bioassay-guided fractionation. Among the fractions obtained from active extracts, only four of ten fractions obtained from the *C. senegalensis* $CHCl_3$-MeOH (9:1, v/v) extract showed a dose-dependent inhibition (supplemental Fig. S2). Chromatographic separation of the most active fraction (fraction E,

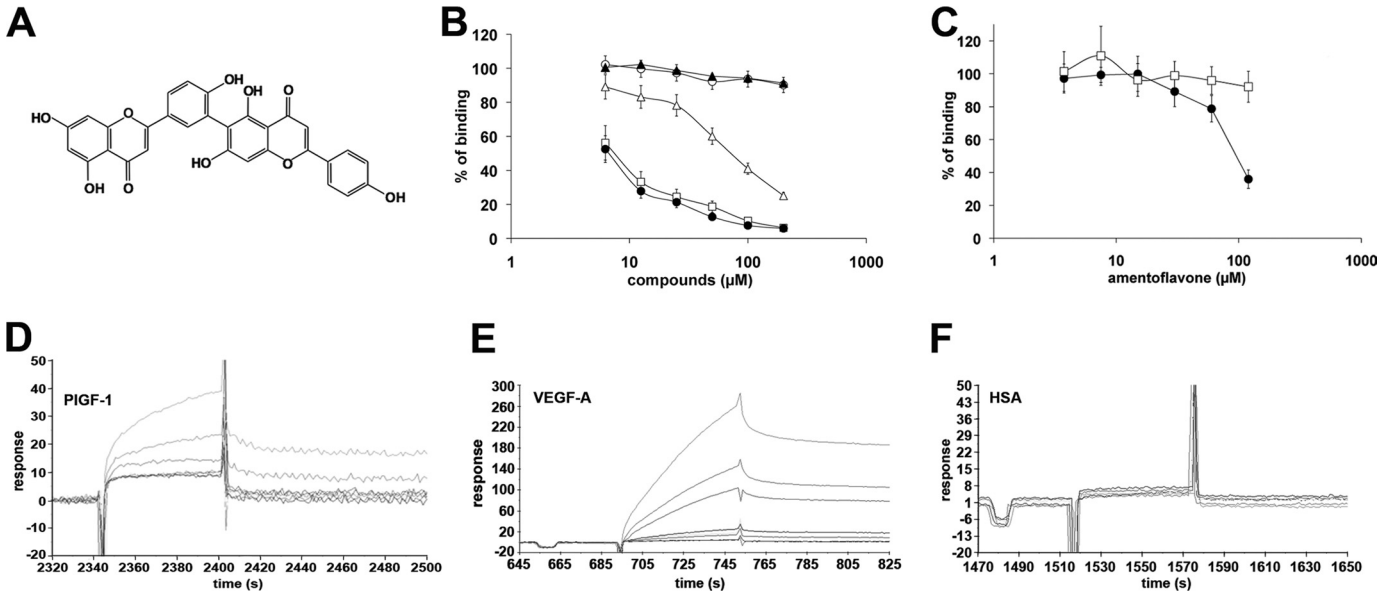

FIGURE 1. **Inhibitory and binding properties of amentoflavone.** *A*, AF structure. *B*, dose-dependent inhibition of the PlGF-1/VEGFR-1 (*filled circles*), VEGF-A/VEGFR-1 (*open squares*), and VEGF-A/VEGFR-2 (*open triangles*) interaction exerted by AF at concentration ranging between 3.75 and 200 μM in ELISA-based assays. As a negative control of inhibition fraction G (supplemental Fig. S2) was used at same concentration for PlGF-1/VEGFR-1 (*filled triangles*) and VEGF-A/VEGFR-2 (*open circles*) interactions. Each point was done in triplicate, and each experiment was repeated twice. Data are represented as the mean ± S.E. *C*, dose-dependent inhibition of VEGF-B/VEGFR-1 (*filled circles*) and PDGF-B/PDGFR-β (*open squares*) interactions exerted by AF at concentration ranging between 3.75 and 200 μM in ELISA-based assays. Each point was done in triplicate, and each experiment was repeated twice. Data are represented as the mean ± S.E. *D–F*, sensograms obtained injecting increasing concentrations (from 0.05 to 10 μM) of AF on PlGF-1-, VEGF-A-, and human serum albumin-coated Biacore chips.

supplemental Fig. S2) by RP-HPLC allowed identification of the main component as the AF at 98.4% purity (supplemental Fig. S1). The AF structure was elucidated by one- and two-dimensional NMR spectroscopy as well as ESI mass spectrometry and comparison with published data (Fig. 1*A* and supplemental data).

Amentoflavone Specifically Inhibits VEGFs Binding to Related Receptors—As shown in Fig. 1*B*, AF inhibited in a similar dose-dependent manner PlGF-1/VEGFR-1 and VEGF-A/VEGFR-1 interactions with an IC_{50} of 4.8 ± 0.3 and 6.8 ± 0.5 μM, respectively. Additionally, it also was able to inhibit the VEGF-A/VEGFR2 interaction but with reduced efficacy (IC_{50} = 104.4 ± 8.4 μM). As negative control, a nonactive fraction from the same extracts (fraction G, supplemental Fig. S2) was used. AF showed similar inhibitory activity also for VEGF-B/VEGFR-1 interaction (IC_{50} = 100.7 ± 7.6 μM) (Fig. 1*C*).

To evaluate the specificity of AF activity, we investigated its inhibitory properties of the interaction between a member of the more structural VEGF-related growth factor family, the PDGF B with related PDGFR-β receptor (PDGFR), and as shown in Fig. 1*C*, no activity was observed.

Amentoflavone Binds VEGFs—To define the molecular target of AF, surface plasmon resonance experiments by Biacore technology were performed. Recombinant PlGF-1, VEGF-A Fc-VEGFR-1 chimera, and as controls, tubulin, and human serum albumin were coated to a Biacore chip and incubated with increasing concentration of AF starting from 0.05 to 10 μM, measuring the association and dissociation to the coated proteins. AF was able to interact with PlGF-1 and VEGF-A, as demonstrated by the concentration-dependent responses and the clearly discernible exponential curves during both the association and dissociation phases (Fig. 1, *D* and *E*). A thermodynamic dissociation constant (K_D) of 16.45 ± 0.59 nM and 8.15 ± 0.28 nM was measured for VEGF-A·AF and the PlGF-1·AF complexes, respectively. No significant interaction was detected with human serum albumin (Fig. 1*F*) or other controls (data not shown). Because AF is a dimer of apigenin (29), we evaluated whether apigenin and structurally related compounds such as quercetin, naringenin, and catechin were able to bind VEGFs, but none of them interacted with PlGF-1 or VEGF-A in surface plasmon resonance experiments (data not shown).

Amentoflavone Prevents VEGF-induced Receptor Activation, Cell Migration, and Capillary-like Tube Formation—The neutralizing activity of AF observed *in vitro* was therefore assessed in receptor phosphorylation assays. AF was able to reduce, in a dose-dependent manner, PlGF-1- and VEGF-A-induced phosphorylation of human VEGFR-1 in the cell line stably overexpressing the receptor (293-hFlt-1) (Fig. 2*A*). Notably, the inhibition activity was higher for VEGF-A-induced VEGFR-1 activation, with an inhibition of ~40% using 2 μM AF ($p <$ 0.005), whereas at 10 μM, the observed inhibition was similar to that obtained with a neutralizing anti-VEGF-A antibody (R&D Systems) used at ~3 nM (~70%, $p < 0.001$). At 25 μM AF, ~90% of inhibition was obtained ($p < 0.0005$). In the VEGFR-1 phosphorylation induced by PlGF-1, AF at 10 μM was able to induce ~50% of inhibition ($p < 0.005$), whereas at 25 μM the extent of inhibition increased up to 75% ($p < 0.0005$).

To evaluate whether AF was able to inhibit also VEGF-A-induced VEGFR-2 phosphorylation, we used primary HUVECs. As shown in Fig. 2*B*, AF also gave a strong dose-dependent inhibition of VEGFR-2 phosphorylation ($p < 0.0005$, $p < 0.001$, and $p < 0.005$ for AF at 25, 10, and 2 μM, respectively).

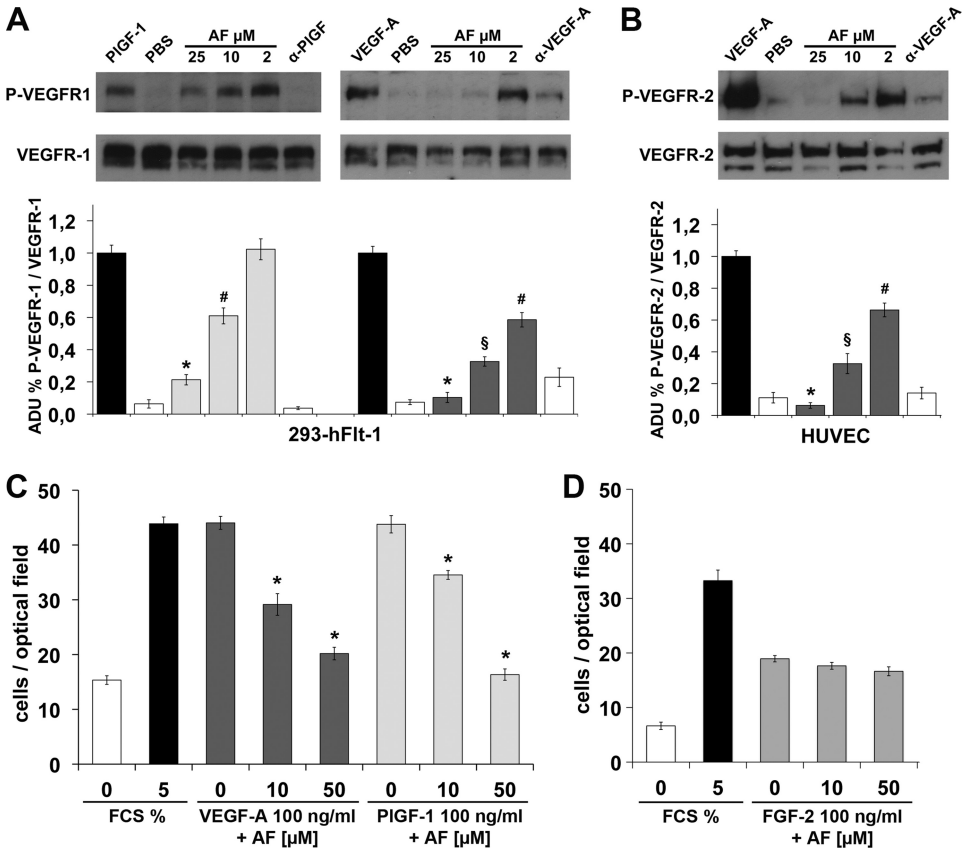

FIGURE 2. **Amentoflavone inhibits VEGFR phosphorylation and HUVEC migration.** *A*, representative pictures of Western blot analysis of VEGFR-1 phosphorylation (P-VEGFR-1) induced by 20 ng/ml of PlGF-1 or 50 ng/ml VEGF-A on cells overexpressing VEGFR-1 (293-Flt-1). AF was used at a concentration ranging between 2 and 25 μM. As control of inhibition neutralizing antibody anti-PlGF (α-PlGF) or anti-VEGF-A (α-VEGF-A) were used at 3.3 nM. Anti-VEGFR-1 antibody was used for normalization. *B*, Western blot analysis of VEGFR-2 phosphorylation (P-VEGFR-2) performed in the same condition as reported in *A* but on HUVECs. Anti-VEGFR-2 antibody was used for normalization. Histograms represent densitometry analysis of three independent experiments, and data are represented as the mean ± S.E. *ADU*, arbitrary densitometric unit. *, $p < 0.0005$ *versus* PlGF-1 or VEGF-A; §, $p < 0.001$ *versus* VEGF-A; #, $p < 0.005$ *versus* PlGF-1 or VEGF-A. *C*, cell migration induced by VEGF-A or PlGF-1 was significantly inhibited by AF used at 10 and 50 μM. Conversely, AF failed to inhibit FGF-2-stimulated cell migration *D*, 0% or 5% FCS were used as negative and positive control of migratory stimulus. *, $p < 0.0001$ *versus* VEGF-A, PlGF-1, and FCS (5%). Each point was done in quadruplicate, and the experiments were performed twice. Data are represented as the mean ± S.E.

Before evaluating further inhibitory activities of AF on endothelial cells, we investigated the toxicity *in vitro* of the molecule evaluating its concentration able to kill 50% of proliferating HUVECs (LD_{50}). The analysis reported in supplemental Fig. S3*A* allowed the calculation of an LD_{50} of 290.0 ± 17.8 μM.

Because cell migration represents one of the crucial events for neovessel formation, we evaluated the effects of AF on HUVEC migration in response to VEGF-A and PlGF-1. Exposure to 10 μM AF for 4 h led to a significant decrease of the migratory movement toward both stimulus ($p < 0.0001$). Moreover, at 50 μM, the number of migrating cells was reduced to that of basal levels ($p < 0.0001$) (Fig. 2*C*). At the same concentrations AF resulted ineffective in inhibiting the HUVEC migratory movement elicited by FGF2 (Fig. 2*D*), further indicating the specificity of AF *versus* VEGFs.

The antiangiogenic activity of AF was evaluated successfully by testing its capability to suppress the induction of capillary-like tube formation (CTF) of HUVECs grown on Matrigel (BD Biosciences) stimulated by PlGF-1, VEGF-A, or FGF2. Endothelial basal medium 2 and complete EGM-2 medium were used as negative and positive controls, respectively (Fig. 3). All growth factors and EGM-2 induced a visible network of capillary-like tube structures with no significant difference in terms of branch points. The suppression of PlGF-1- and VEGF-A-induced CTF by AF was virtually complete at 20 μM ($p < 0.0005$ *versus* VEGF-A, PlGF-1 and EGM-2), with a number of branch points similar to that of the negative control. At 2 μM AF, the great part of tube network was absent with a reduction of >50% of branch points ($p < 0.003$ *versus* VEGF-A, and EGM-2; $p < 0.01$ *versus* PlGF-1, and EGM-2). AF was not able to inhibit FGF-2-induced CTF when assayed at 20 and 50 μM, as well as the CTF induced by complete EGM-2 medium (Fig. 3). These latter data confirm that AF possesses a specific activity toward VEGFs and that it does not have a direct effect on endothelial cells.

In Vivo Antiangiogenic Activity of Amentoflavone—The antiangiogenic activity of AF was investigated in the model of chicken embryo chorioallantoic membrane assay. VEGF-A at 50 ng/ml determined a good increment of vessel formation compared with vehicle alone (Fig. 4). AF addressed VEGF-A-induced angiogenesis in all of the embryos tested showing a significant dose-response inhibition. One μg (1.9 nmol) of AF was sufficient to achieve ~50% of inhibition ($p < 0.01$), whereas in the presence of 5 μg (9.5 nmol), the number of neovessels was similar to that observed with vehicle alone ($p < 0.001$) (Fig. 4). Therefore, AF was able to abolish the stimulation of VEGF-A

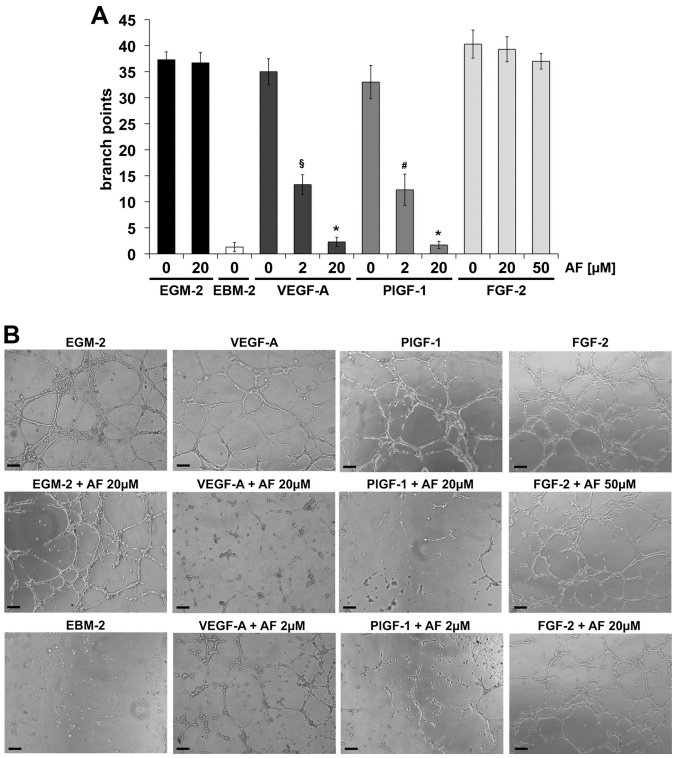

FIGURE 3. **Amentoflavone inhibits capillary-like tube formation induced by VEGF-A or PlGF-1 but not by FGF-2.** *A*, CTF stimulated with 100 ng/ml of VEGF-A, PlGF-1, or FGF-2 in presence or absence of AF, used at concentrations ranging between 2 and 50 μM. Branch points for almost three capillary-like structures have been quantified in three optical fields for each sample. Data are represented as the mean ± S.E. §, $p < 0.003$ *versus* VEGF-A, and EGM-2; #, $p < 0.01$ *versus* PlGF-1, and EGM-2; *, $p < 0.0005$ *versus* VEGF-A, PlGF-1, and EGM-2. *B*, representative pictures. The *scale bar* represents 100 μm.

without affecting pre-existing vessels. Finally, the antiangiogenic property of AF was evaluated in an orthotopic model of melanoma and a xenograft model of colon carcinoma.

First, we assessed whether AF affected *per se* the proliferation *in vitro* of the two cell lines used for tumor models, MeWo melanoma and HCT-116 colon carcinoma cells. As shown in supplemental Fig. S3, *B* and *C*, AF did not affect cell proliferation when assayed at concentrations ranging between 6.25 and 50 μM.

MeWo melanoma cells were injected intradermally in nude mice. Three days after, AF dissolved in 1% gum acacia was daily delivered intraperitoneally at 50 mg/10 ml/kg (27). After 14 days from cell injection, AF gave a significant and homogenous tumor volume reduction (−63%, $p = 0.0005$ *versus* vehicle) despite the short dimension of control tumors (~60 mg), to which a significant reduction of vessel density corresponded (−52,5%, $p = 0.0051$ *versus* vehicle), as assessed by CD31 immunohistochemical analysis (Table 1 and Fig. 5*A*).

The immunohistochemical analysis, performed to evaluate the tumor infiltration by F4/80 positive cells, clearly indicated a significant inhibition of their recruitment (−41%, $p < 0.0001$ *versus* vehicle) (Table 1 and Fig. 5*A*), as expected due to the crucial role of both VEGF-A and PlGF-1 in this biological activity exerted mainly via activation of VEGFR-1.

HCT-116 colon carcinoma cells were injected subcutaneously in nude mice. In this case, AF was delivered when tumors became measurable (50–100 mm^3) after 7 days from cell inoculation using the same delivery schedule described for melanoma model. After 7 days of treatment with AF, a significant inhibition of tumor growth in mice became measurable (−34%,

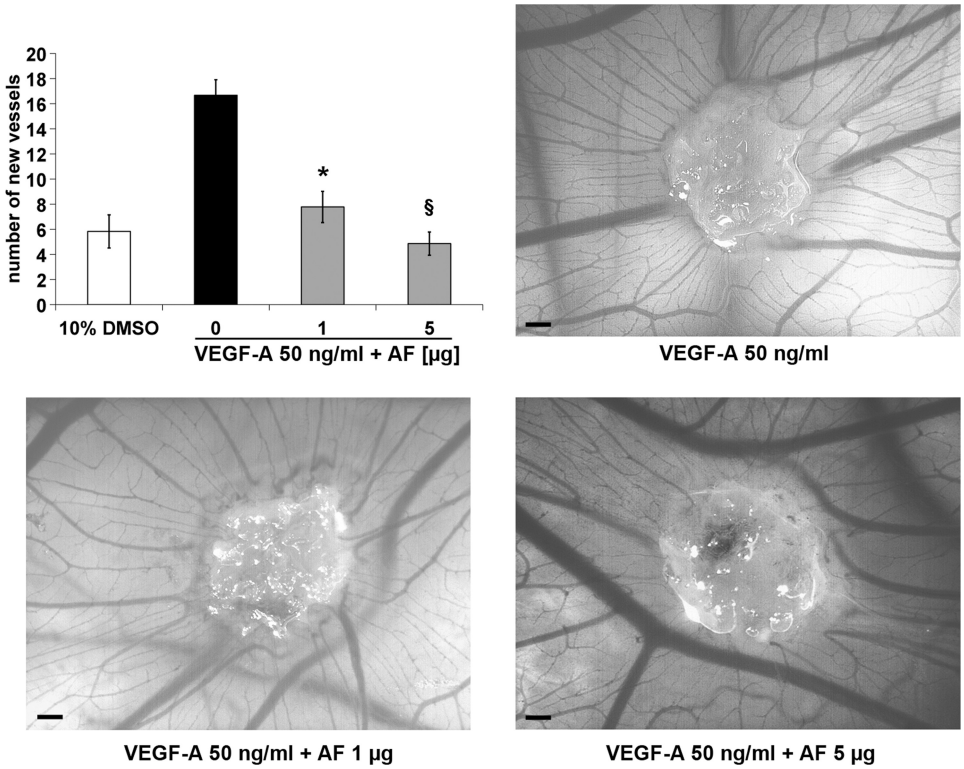

FIGURE 4. **Amentoflavone inhibits VEGF-A-induced chorioallantoic membrane neovascularization.** Inhibition of VEGF-A-induced neovessels formation exerted by AF (1 and 5 μg). The vehicle used was 10% dimethyl sulfoxide (DMSO; $n = 8$ per group). Data are represented as the mean ± S.E. *, $p < 0.01$ and §, $p < 0.001$ *versus* VEGF-A treated embryos. The *scale bar* represents 200 μm.

TABLE 1

***In vivo* antitumor activity of AF on human MeWo melanoma**

MeWo tumor cells (5×10^5) were injected i.d. in CD1 nude mice. Test compound was given i.p. starting 3 days after tumor implantation to day 13. TV (tumor volume) was evaluated at day 14. The vessel number and F4/80-positive area were determined in five optical fields for each tumor. Data represent the average ± S.E. BW, body weight.

Group	Dose (mg/kg/BW)	Lethality	TV (mm^3)	Vessels/mm^2	F4/80 positive area/mm^2
Vehicle	0	0/9	57.2 ± 8.2	112.5 ± 14.5	8.1 ± 0.4
AF	50	0/9	21.4 ± 0.5[a]	53.5 ± 11.0[b]	4.8 ± 0.3[c]

[a] $p = 0.0005$.
[b] $p = 0.0051$.
[c] $p < 0.0001$ *versus* vehicle.

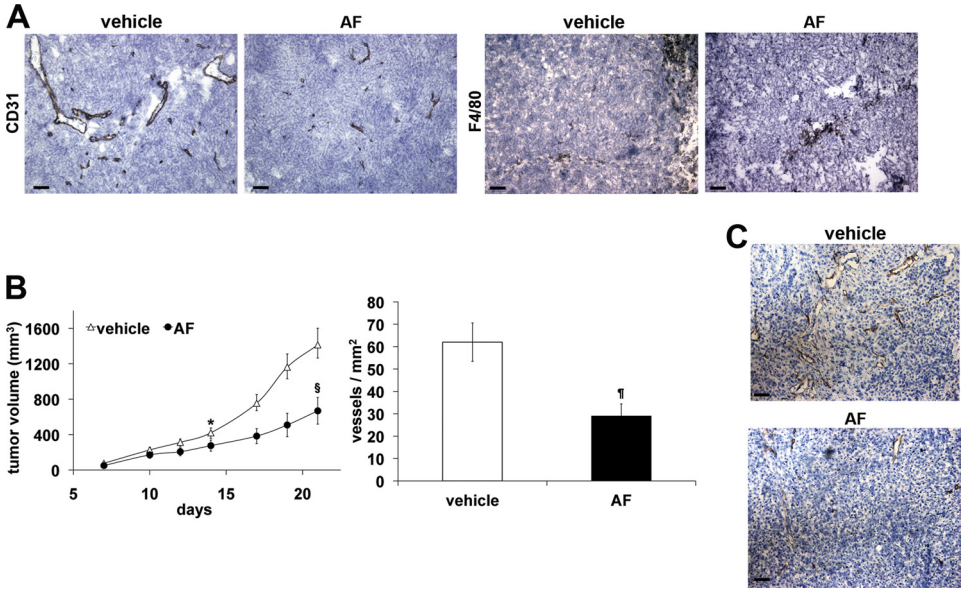

FIGURE 5. **Amentoflavone inhibits tumor growth and associated neovascularization.** *A*, representative pictures of CD31 and F4/80 staining of MeWo melanoma (see Table 1). *B*, HCT-116 xenograft tumor volume was measured three times a week, and data are represented as the mean ± S.E. *, $p = 0.0109$; §, $p = 0.0078$ *versus* vehicle. Vessel density was calculated analyzing five optical fields for each tumor, counting CD31-positive vessels. Data are represented as the mean ± S.E. ¶, $p = 0.0070$ *versus* vehicle. *C*, representative pictures of CD31 staining of HCT-116 tumors. The *scale bar* represents 50 μm.

$p = 0.0109$ *versus* vehicle) (Fig. 5*B*). At day 21 from cell inoculation, the reduction of tumor growth increased to 53% ($p = 0.0078$ *versus* vehicle) and the immunohistochemical analysis for CD31 performed on explanted tumors allowed to associate a significant vessel density decrease (−53%, $p = 0.0070$) to reduced tumor growth (Fig. 5*B*, *C*). In course of the treatment in both tumor models, no side effects were noted except for a reduction of mice body weight (between 6–8% at the experimental end point).

Structural Characterization of PlGF-1·AF Complex—To unveil the nature and the characteristics of AF binding to soluble proangiogenic factors, we started a structural characterization focusing our attention on the PlGF-1·AF complex because it showed the highest stability. We first performed a circular dichroism analysis. The near-UV circular dichroism spectroscopy demonstrated that binding of AF to PlGF-1 produces a large change in the spectrum of the protein, thus suggesting a rearrangement of its tertiary structure (supplemental data and Fig. S4, *A* and *B*). On the other hand, ESI-MS analyses suggested a noncovalent interaction because the acquired spectra for PlGF-1·AF complex was almost identical to that of PlGF-1 alone (supplemental Fig. S4*C*).

To identify the PlGF-1 protein regions involved in the interaction with AF, structural studies were performed starting from the noncovalent PlGF-1·AF complex. As a first analytical step, we attempted to transform the noncovalent interaction in a stable bond by UV cross-linking reaction. Since the phenol group was the unique functional group of AF reactive enough, we used the phenol reactive-NHS-diaziridine as photoactivable reagent. The complex stabilized by cross-linking was detectable by linear MALDI-TOF analysis (supplemental Fig. S5). Therefore, it was subjected to trypsin cleavage. The comparison analysis of digested peptides performed by MALDI-TOF/TOF analysis (supplemental Fig. S6, *A* and *B*) revealed that the peptide-(94–110) and peptide-(125–132) were modified after the cross-linking reaction (supplemental Table S2). We did not observe complex formation if the same experiment was performed using two structurally related compounds (catechin and quercetin), which showed no binding toward VEGFs (supplemental Fig. S7).

As a second approach, limited proteolysis experiments coupled with mass spectrometry analysis were carried out to probe the conformational changes of proteins induced by ligand binding and to map the interface regions protected from the access of protease by the molecular interaction (30). A comparison among the digestion patterns observed when PlGF-1 or PlGF-1·AF noncovalent complex underwent proteolytic digestion using different enzymes, demonstrated that the residues mainly protected by AF against proteolysis were as follows: Leu-2, which was miscleaved by chymotrypsin, Lys-119 and Arg-131 were protected from trypsin cleavage; Glu-123, which was not cleaved by endoproteinase Glu-C (Prot. V8); and residues

TABLE 2

Role of PlGF-1 core residues involved in the interaction with AF, as elicited by structural analyses and docking model

LP, Limited Proteolysis; UVcl, UV cross-linking; Dock: docking. For the nature of interactions, PlGF-1/VEGFR-1 and the data reported in the last column (the numbers in parentheses represent the number of contacts with the VEGFR-1 residues indicated), see Ref. 31. For the decrease affinity by mutation in Ala, see Ref. 25.

PlGF residues	Type of analysis	Residues at 6 Å from AF (type of interaction)	Nature of interactions PlGF/VEGFR-1	Affinity decrease by mutation in Ala	VEGFR-1_{D2} putative intermolecular contacts
Pro-25	Dock			25%	
Phe-26	Dock	aromatic π-π	Van der Waals		Pro-143(2), Leu-221(2)*
Gln-27	LP + Dock		polar	50%	Glu-141(3), Ile-142, Pro-143(9), Leu-204, Asn-219(3)
Gln-88	Dock	H-π	Van der Waals		Ile-142
Arg-97	UVcl + Dock				
Pro-98	UVcl + Dock	H-bond (C7-OH group)		50%	
Ser-99	UVcl + Dock	H-π			
Tyr-100	UVcl + Dock	aromatic π-π	Van der Waals + polar	25%	Ile-142(10), Pro-143(2)

Gln-27 and Arg-32, which were protected when endoproteinase PK was used (supplemental Table S3 and supplemental Fig. S8).

The peptide-(94–110) and residues Gln-27 and Arg-32, highlighted by cross-linking and limited proteolysis analyses, respectively, belong to the structural core of PlGF crucial for VEGFR-1 recognition (residues 18–117) (31). Some of these residues are involved in receptor binding (Table 2). Therefore, these results suggest that AF is effectively able to mask some PlGF-1 residues that are involved in receptor recognition.

DISCUSSION

Flavonoids are a class of natural compounds belonging to the large polyphenolic family widely distributed in the plant kingdom displaying a variety of biological effects like antioxidant, antiviral, and anti-inflammatory activities. In the past few years, the interest on these compounds has increased because they displayed potentiality not only as cancer-chemopreventive but also as cancer therapeutic natural agents. It has been reported that these compounds are able to modulate proteins activity acting on multiple key elements of signal transduction pathways involved in cell proliferation, differentiation, apoptosis, in angiogenesis, and inflammation, determining cancer growth inhibition. However, these mechanisms of action have not been fully characterized, and many features remain to be elucidated (32–34).

Here, we have reported the screening of a large collection of plant extracts based on the idea to identify small molecules able to prevent the initial event needed for the proangiogenic activity of the VEGF family members, the interaction of VEGF-A, PlGF-1, and VEGF-B with VEGFR-1 and VEGFR-2 receptors.

As a result, we were able to isolate AF from an extract of the Malian plant *C. senegalensis* as an antiangiogenic bioactive molecule. Indeed, we have demonstrated that AF is able to bind VEGF-A and PlGF-1 preventing the interaction and consequent phosphorylation of VEGFR-1 and VEGFR-2, as well as endothelial cell migration and CTF induced by either protein. It also inhibits the *in vitro* VEGF-B/VEGFR-1 interaction. Interestingly, AF did not inhibit the activity of other homodimeric proteins involved in neovessel formation and stabilization such as PDGF, structurally related to VEGFs and FGF because it fails to block *in vitro* PDGF-B/PDGFR-β interaction and FGF-2-induced chemotaxis and CTF. These results indicate how AF possesses a binding specificity for VEGF family members acting at the low micromolar concentration range, therefore widely distant from its cytotoxic concentration.

In vivo, AF is able to inhibit VEGF-induced chorioallantoic membrane neovascularization. Finally, we evaluated its antitumor effects on two different cancer experimental models: an orthotropic model of melanoma and a xenograft model of colon carcinoma. AF, daily delivered intraperitoneally at 50 mg/kg, was able to inhibit tumor growth and associated neoangiogenesis in a significant manner in both models.

AF belongs to a unique class of naturally occurring biflavonoids and is able to exert the general properties of flavonoids (35–38). More recently, its antiangiogenic effect has been described in an assay of tumor-directed capillary formation using a melanoma model generated via subcutaneous injection of B16-F10 melanoma cells. AF delivered simultaneously with tumor cell inoculation for 5 days, determined a significant inhibition of tumor directed neovessels, as observed 9 days after cell injection. The authors reported an altered proinflammatory circulating cytokines production as well as reduction of circulating VEGF-A as possible explanation of AF action (27).

These results may be fully accounted for by considering the mechanism of action that we have discovered, which has never been reported before. Indeed, the AF ability to interact with proangiogenic VEGF family members preventing their binding to VEGF receptors is crucial for the observed inhibition of new vessel formation, as direct effect on endothelial cells proliferation, migration, and differentiation, in which both proangiogenic VEGF growth factors and VEGF receptors are involved.

Moreover, inflammation is strictly associated with tumor angiogenesis and growth and is able to sustain neoangiogenesis. PlGF and VEGF-A play a crucial role in the recruitment of inflammatory cells at neoangiogenic site (17), mainly interacting with VEGFR-1 expressed on their surfaces (39, 40), as demonstrated by the inhibition of F4/80 positive cells recruitment observed in AF treated melanoma. This reduction may be responsible, almost in part, for the reported decrease of general proinflammatory circulating cytokines. Moreover, this reduction, together with reduced tumor growth, also explains the decrease of circulating VEGF-A because it is mainly produced by tumor cells and by recruited myeloid cells such as monocyte macrophages. Nonetheless, we cannot exclude that AF may exert its action also modulating proinflammatory cytokines by alternative pathways.

From a structural point of view, AF is an apigenin dimer. Many data have been reported on the antiangiogenic and antitumoral action of apigenin, in particular for its ability to interfere with hypoxia-inducible factor-1α activity and expression

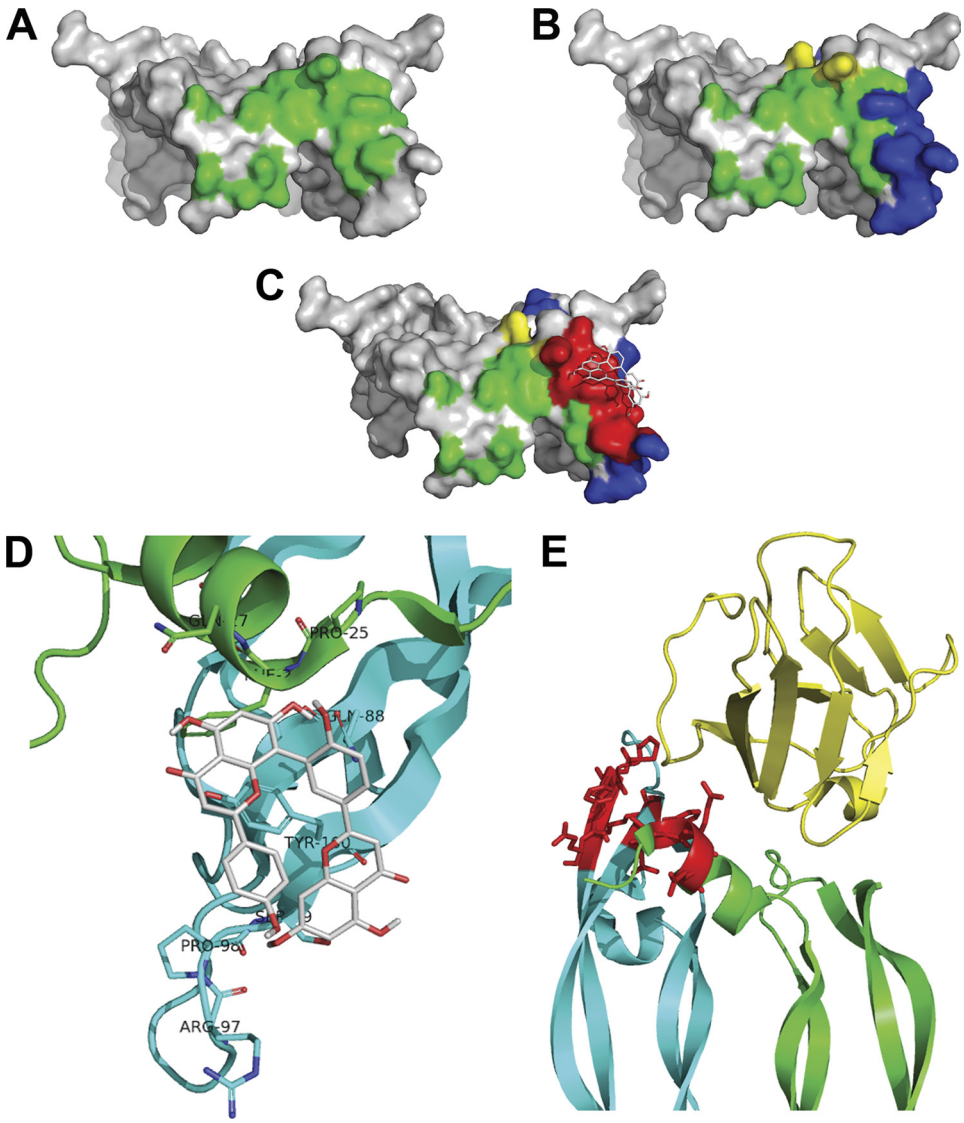

FIGURE 6. **Docking analysis of PlGF-1·amentoflavone complex.** Shown is a surface plot of PlGF-1 showing the residues involved in Flt-1 recognition in *green* (*A*), the peptide-(94–110), identified by UV cross-linking analysis, and the residues Gln-27 and Arg-32, evidenced with limited proteolysis analysis, highlighted in *blue* and *yellow*, respectively (*B*). *C*, surface plot of the model of the PlGF-1·AF complex showing the lowest binding energy. *Red* indicates the area within 6 Å from the ligand. A high overlapping with *blue* and *green* residues was observed. *D*, magnification of interaction area between AF and PlGF-1. The PlGF-1 residues of the two monomers (*green* and *cyan*) involved in AF interaction are indicated. AF and side chains of PlGF-1 residues involved in contacts are represented as *sticks* with colored atoms (*white*, hydrogen; *red*, oxygen; *blue*, nitrogen). *E*, the PlGF-1·VEGFR-1 D2 complex (Protein Data Bank code 1RV6) is shown with the two monomers of PlGF-1 homodimer represented in *green* and *cyan*, and the VEGFR-1 D2 domain is represented in *yellow*, whereas the PlGF-1 residues and corresponding side chains at 6 Å from AF inhibitor are highlighted in *red*.

(41, 42). Interestingly, neither apigenin nor related molecules as quercetin, naringenin, and catechin are able to interact with VEGFs, as assessed by surface plasmon resonance assays. Consequently, the binding properties and activity of AF strictly depends on their own structural features and not on general flavonoid characteristics.

Data generated by cross-linking and limited proteolysis clearly indicated the capability of AF to interact in the area of PlGF-1 involved in the recognition of the receptor. Indeed, the residue Gln-27 highlighted with limited proteolysis analysis is involved in polar interaction with VEGFR-1 (31). The relevance of this residue in the PlGF-1·VEGFR-1 complex stabilization was demonstrated previously also with mutagenesis studies, which indicated that its mutation in Ala was sufficient to decrease to 50% the PlGF-1 binding activity to the receptor (25). Among the residues of the peptide-(94–110) evidenced by UV cross-linking, the residue Tyr-100 is involved in both van der Waals and polar interactions with VEGFR-1. Mutagenesis studies indicated that its mutation in Ala, as well as that of the residue Pro-98, determined a decrease of 25 or of 50% of PlGF-1 binding activity to the receptor, respectively (Table 2) (25, 31).

To better understand the mechanism of interaction between AF and PlGF-1, these data have been used to generate a preliminary model of PlGF-1·AF complex using the docking approach (Fig. 6*C*) (43, 44). The atomic coordinates and three-dimensional structure of recombinant PlGF-1 homodimer used for calculations were based on crystallographic structure of PlGF-1 (Protein Data Bank code 1FZV) (31).

PlGF-1 residues Pro-25, Phe-26, and Gln-27 from one monomer and Gln-88, Arg-97, Pro-98, Ser-99, and Tyr-100 from the

other monomer all localized in the area involved in VEGFR-1 recognition (Fig. 6, *D* and *E*), were found at 6 Å from the inhibitor (25, 31, 45). According to this model, the interaction between PlGF-1 and AF is mainly hydrophobic (Table 2). Docking of the nonactive flavonoid catechin performed with identical parameters showed an interaction involving a protein region clearly different from that observed for AF and not implicated in the VEGFR-1 recognition (supplemental Fig. S9).

Docking results furtherly support the role of PlGF-1 residues highlighted with cross-linking and limited proteolysis analyses. In addition, the three residues Pro-25, Phe-26, and Gln-27 are part of the PlGF-1 α1-helix, a structural element crucial for the stabilization of PlGF-1 dimer (31, 45). Moreover, the residues Phe-26 and Gln-88 are involved in van der Waals interactions with the VEGFR-1 receptor, whereas mutagenesis of Pro-25 in Ala determined a 25% reduction of PlGF-1 binding activity to the receptor (Table 2 and supplemental Fig. S10) (25, 31).

Altogether, these data suggest how AF is able to interact with PlGF-1 residues that play a crucial role in receptor recognition. Moreover, additional structural studies are needed to identify the residues of VEGF-A and VEGF-B involved in AF binding to correctly evaluate how this interaction may affect the receptor recognition.

In conclusion, the data here reported demonstrate that AF possesses antiangiogenic activity due to its ability to selectively bind proangiogenic VEGF family members, preventing their interaction with VEGF receptors. Therefore, we propose that AF may be considered as a promising new chemical scaffold to develop, by medicinal chemistry approaches, powerful new small molecules for the inhibition of pathological neoangiogenesis.

Acknowledgments—We thank Professor D. Collen, Chairman of the D. Collen Research Foundation, for support; Vincenzo Mercadante and all the staff of IGB animal house for technical assistance; Andrea Lorentzen for assistance in acquisition of data on the 4800 instrument; and Anna Maria Aliperti for manuscript editing.

REFERENCES

1. Ferrara, N., Gerber, H. P., and LeCouter, J. (2003) *Nat. Med.* **9,** 669–676
2. Carmeliet, P. (2005) *Nature* **438,** 932–936
3. De Falco, S., Gigante, B., and Persico, M. G. (2002) *Trends Cardiovasc. Med.* **12,** 241–246
4. Ferrara, N., Hillan, K. J., and Novotny, W. (2005) *Biochem. Biophys. Res. Commun.* **333,** 328–335
5. Gragoudas, E. S., Adamis, A. P., Cunningham, E. T., Jr., Feinsod, M., and Guyer, D. R. (2004) *N. Engl. J. Med.* **351,** 2805–2816
6. Rosenfeld, P. J., Brown, D. M., Heier, J. S., Boyer, D. S., Kaiser, P. K., Chung, C. Y., and Kim, R. Y. (2006) *N. Engl. J. Med.* **355,** 1419–1431
7. Ellis, L. M., and Hicklin, D. J. (2008) *Nat. Rev. Cancer* **8,** 579–591
8. Wu, Y., Zhong, Z., Huber, J., Bassi, R., Finnerty, B., Corcoran, E., Li, H., Navarro, E., Balderes, P., Jimenez, X., Koo, H., Mangalampalli, V. R., Ludwig, D. L., Tonra, J. R., and Hicklin, D. J. (2006) *Clin Cancer Res.* **12,** 6573–6584
9. Fischer, C., Jonckx, B., Mazzone, M., Zacchigna, S., Loges, S., Pattarini, L., Chorianopoulos, E., Liesenborghs, L., Koch, M., De Mol, M., Autiero, M., Wyns, S., Plaisance, S., Moons, L., van Rooijen, N., Giacca, M., Stassen, J. M., Dewerchin, M., Collen, D., and Carmeliet, P. (2007) *Cell* **131,** 463–475
10. Van de Veire, S., Stalmans, I., Heindryckx, F., Oura, H., Tijeras-Raballand, A., Schmidt, T., Loges, S., Albrecht, I., Jonckx, B., Vinckier, S., Van Steenkiste, C., Tugues, S., Rolny, C., De Mol, M., Dettori, D., Hainaud, P., Coenegrachts, L., Contreres, J. O., Van Bergen, T., Cuervo, H., Xiao, W. H., Le Henaff, C., Buysschaert, I., Kharabi Masouleh, B., Geerts, A., Schomber, T., Bonnin, P., Lambert, V., Haustraete, J., Zacchigna, S., Rakic, J. M., Jiménez, W., Noël, A., Giacca, M., Colle, I., Foidart, J. M., Tobelem, G., Morales-Ruiz, M., Vilar, J., Maxwell, P., Vinores, S. A., Carmeliet, G., Dewerchin, M., Claesson-Welsh, L., Dupuy, E., Van Vlierberghe, H., Christofori, G., Mazzone, M., Detmar, M., Collen, D., and Carmeliet, P. (2010) *Cell* **141,** 178–190
11. Carmeliet, P., Moons, L., Luttun, A., Vincenti, V., Compernolle, V., De Mol, M., Wu, Y., Bono, F., Devy, L., Beck, H., Scholz, D., Acker, T., DiPalma, T., Dewerchin, M., Noel, A., Stalmans, I., Barra, A., Blacher, S., Vandendriessche, T., Ponten, A., Eriksson, U., Plate, K. H., Foidart, J. M., Schaper, W., Charnock-Jones, D. S., Hicklin, D. J., Herbert, J. M., Collen, D., and Persico, M. G. (2001) *Nat. Med.* **7,** 575–583
12. Luttun, A., Tjwa, M., Moons, L., Wu, Y., Angelillo-Scherrer, A., Liao, F., Nagy, J. A., Hooper, A., Priller, J., De Klerck, B., Compernolle, V., Daci, E., Bohlen, P., Dewerchin, M., Herbert, J. M., Fava, R., Matthys, P., Carmeliet, G., Collen, D., Dvorak, H. F., Hicklin, D. J., and Carmeliet, P. (2002) *Nat. Med.* **8,** 831–840
13. Rakic, J. M., Lambert, V., Devy, L., Luttun, A., Carmeliet, P., Claes, C., Nguyen, L., Foidart, J. M., Noël, A., and Munaut, C. (2003) *Invest. Ophthalmol. Vis. Sci.* **44,** 3186–3193
14. Kaplan, R. N., Riba, R. D., Zacharoulis, S., Bramley, A. H., Vincent, L., Costa, C., MacDonald, D. D., Jin, D. K., Shido, K., Kerns, S. A., Zhu, Z., Hicklin, D., Wu, Y., Port, J. L., Altorki, N., Port, E. R., Ruggero, D., Shmelkov, S. V., Jensen, K. K., Rafii, S., and Lyden, D. (2005) *Nature* **438,** 820–827
15. Gigante, B., Morlino, G., Gentile, M. T., Persico, M. G., and De Falco, S. (2006) *FASEB J.* **20,** 970–972
16. Cao, Y. (2009) *Sci. Signal* **2,** re1
17. Tarallo, V., Vesci, L., Capasso, O., Esposito, M. T., Riccioni, T., Pastore, L., Orlandi, A., Pisano, C., and De Falco, S. (2010) *Cancer Res.* **70,** 1804–1813
18. Fischer, C., Mazzone, M., Jonckx, B., and Carmeliet, P. (2008) *Nat. Rev. Cancer* **8,** 942–956
19. Newman, D. J., Cragg, G. M., and Snader, K. M. (2003) *J. Nat. Prod.* **66,** 1022–1037
20. Ponticelli, S., Braca, A., De Tommasi, N., and De Falco, S. (2008) *Planta Med.* **74,** 401–406
21. Ponticelli, S., Marasco, D., Tarallo, V., Albuquerque, R. J., Mitola, S., Takeda, A., Stassen, J. M., Presta, M., Ambati, J., Ruvo, M., and De Falco, S. (2008) *J. Biol. Chem.* **283,** 34250–34259
22. Kim, H. P., Park, H., Son, K. H., Chang, H. W., and Kang, S. S. (2008) *Arch. Pharm. Res.* **31,** 265–273
23. Maglione, D., Guerriero, V., Viglietto, G., Ferraro, M. G., Aprelikova, O., Alitalo, K., Del Vecchio, S., Lei, K. J., Chou, J. Y., and Persico, M. G. (1993) *Oncogene* **8,** 925–931
24. Dal Piaz, F., Vassallo, A., Lepore, L., Tosco, A., Bader, A., and De Tommasi, N. (2009) *J. Med. Chem.* **52,** 3814–3828
25. Errico, M., Riccioni, T., Iyer, S., Pisano, C., Acharya, K. R., Persico, M. G., and De Falco, S. (2004) *J. Biol. Chem.* **279,** 43929–43939
26. Marcellini, M., De Luca, N., Riccioni, T., Ciucci, A., Orecchia, A., Lacal, P. M., Ruffini, F., Pesce, M., Cianfarani, F., Zambruno, G., Orlandi, A., and Failla, C. M. (2006) *Am J. Pathol.* **169,** 643–654
27. Guruvayoorappan, C., and Kuttan, G. (2008) *Biochemistry* **73,** 209–218
28. Gillet, A., Sanner, M., Stoffler, D., and Olson, A. (2005) *Structure* **13,** 483–491
29. Patel, D., Shukla, S., and Gupta, S. (2007) *Int. J. Oncol.* **30,** 233–245
30. Renzone, G., Salzano, A. M., Arena, S., D'Ambrosio, C., and Scaloni, A. (2007) *Curr. Proteomics* **4,** 1–16
31. Iyer, S., Leonidas, D. D., Swaminathan, G. J., Maglione, D., Battisti, M., Tucci, M., Persico, M. G., and Acharya, K. R. (2001) *J. Biol. Chem.* **276,** 12153–12161
32. Yang, C. S., Landau, J. M., Huang, M. T., and Newmark, H. L. (2001) *Annu. Rev. Nutr.* **21,** 381–406
33. Albini, A., Noonan, D. M., and Ferrari, N. (2007) *Clin. Cancer Res.* **13,** 4320–4325
34. Ramos, S. (2008) *Mol. Nutr. Food Res.* **52,** 507–526

35. Cholbi, M. R., Paya, M., and Alcaraz, M. J. (1991) *Experientia* **47,** 195–199
36. Kim, H. K., Son, K. H., Chang, H. W., Kang, S. S., and Kim, H. P. (1998) *Arch. Pharm. Res.* **21,** 406–410
37. Lin, Y. M., Flavin, M. T., Schure, R., Chen, F. C., Sidwell, R., Barnard, D. L., Huffman, J. H., and Kern, E. R. (1999) *Planta Med.* **65,** 120–125
38. Ma, S. C., But, P. P., Ooi, V. E., He, Y. H., Lee, S. H., Lee, S. F., and Lin, R. C. (2001) *Biol. Pharm. Bull* **24,** 311–312
39. Clauss, M., Weich, H., Breier, G., Knies, U., Röckl, W., Waltenberger, J., and Risau, W. (1996) *J. Biol. Chem.* **271,** 17629–17634
40. Sawano, A., Iwai, S., Sakurai, Y., Ito, M., Shitara, K., Nakahata, T., and Shibuya, M. (2001) *Blood* **97,** 785–791
41. Osada, M., Imaoka, S., and Funae, Y. (2004) *FEBS Lett.* **575,** 59–63
42. Fang, J., Xia, C., Cao, Z., Zheng, J. Z., Reed, E., and Jiang, B. H. (2005) *FASEB J.* **19,** 342–353
43. Lengauer, T., and Rarey, M. (1996) *Curr. Opin. Struct. Biol.* **6,** 402–406
44. van Dijk, A. D., Boelens, R., and Bonvin, A. M. (2005) *FEBS J.* **272,** 293–312
45. Christinger, H. W., Fuh, G., de Vos, A. M., and Wiesmann, C. (2004) *J. Biol. Chem.* **279,** 10382–10388